Environmental Systems Research

RESEARCH Open Access

Modeling of land use and land cover changes using google earth engine and machine learning approach: implications for landscape management

Weynshet Tesfaye[1,2*], Eyasu Elias[2], Bikila Warkineh[4], Meron Tekalign[2] and Gebeyehu Abebe[3]

Abstract

A precise and up-to-date Land Use and Land Cover (LULC) valuation serves as the fundamental basis for efficient land management. Google Earth Engine (GEE), with its numerous machine learning algorithms, is now the most advanced open-source global platform for rapid and accurate LULC classification. Thus, this study explores the dynamics of the LULC changes between 1993 and 2023 using Landsat imagery and the machine learning algorithms in the Google Earth Engine (GEE) platform. Focus group discussion and key informant interviews were also used to get further data regarding LULC dynamics. Support Vector Machine (SVM), Random Forest (RF), and Classification and Regression Trees (CART) were demonstrated for LULC classification. Six LULC types (agricultural land, grazingland, shrubland, built-up area, forest and bareland) were identified and mapped for 1993, 2003, 2013, and 2023. The overall accuracy and kappa coefficient demonstrated that the RF using images comprising auxiliary variables (spectral indices and topographic data) performed better than SVM and CART. Despite being the most common type of LULC, agricultural land shows a trend of shrinking during the study period. The built-up area and bareland exhibits a trend of progressive expansion. The amount of forest and shrubland has decreased over the last 20 years, whereas grazinglands have exhibited expanding trends. Population growth, agricultural land expansion, fuelwood collection, charcoal production, built-up areas expansion, illegal settlement and intervention are among causes of LULC shifts. This study provides reliable information about the patterns of LULC in the Robit watershed, which can be used to develop frameworks for watershed management and sustainability.

Keywords Auxiliary variables, Google Earth Engine, Land use and land cover, Random forest (RF), Robit Watershed

*Correspondence:
Weynshet Tesfaye
tesfayeweynshet19@gmail.com
[1]Department of Biology, Dire Dawa University, Dire Dawa, Ethiopia
[2]Center for Environmental Science, Addis Ababa University, P.O. Box 1176, Addis Ababa, Ethiopia
[3]Department of Natural Resources Management, Debre Berhan University, Debre Berhan, Ethiopia
[4]Department of Plant Biology and Biodiversity Management, Addis Ababa University, Addis Ababa, Ethiopia

Introduction

Land is an important natural resource that provides for most human supplies and sustains most human activity. Despite this, the increasing human population (Obeidat et al. 2019) has brought this natural resource under constant threat by intensifying changes in land cover and use (LULC) over time. LULC change refers to modifications and shifts in the earth's surface cover primarily caused by human activities (Johnson and Zuleta 2013). Anthropogenic LULC changes are more pronounced in tropical areas because of the rapid rates of deforestation, increased agricultural production, industrial development, migration, urbanization, and population density growth (Yeshaneh et al. 2013; Kleemann et al., 2017; Pereira and Tsikata, 2021). The sub-Saharan Africa (SSA) region in particular is predicted to be particularly vulnerable to the effects of LULC shifts as this region experiences a varied pattern of LULC dynamics and notable conversions of forest into agriculture (Obeidat et al. 2019). Ethiopia is also undergoing asymmetrical LULC changes due to its rapidly growing population, which allows cultivated land dominancy and a rapid increase settlement (Tolessa et al., 2016; Nigussie et al. 2017; Tesfay et al. 2022; Gitima et al. 2022; Negash et al. 2023). However, in a few regions of the country, new plantations and the expansion of urban areas onto agricultural land have been shown to be the cause of a growing trend in vegetation and a decreasing trend in farmland (Nigussie et al. 2017; Tesfay et al. 2022; Negash et al. 2023). Varying outcomes might be related to various socioeconomic and biophysical factors (Birhane et al., 2019; Gitima et al. 2022).

LULC shifts have a critical role in altering the microclimate, biodiversity, ecosystem services, hydrological and ecological cycles, and biotic processes of the Earth that negatively impact socioeconomic and sustainable livelihood elements (Abd et al., 2020; Winkler et al. 2021; Negash et al. 2023). In Ethiopia, it appears that LULC changes have increased the amount of degraded land, soil erosion, sedimentation, and nutrient loads into water bodies (Kidane et al. 2019). Monitoring and mitigation of adverse effects resulting from LULC changes has gained global attention from researchers and policymakers (Yuh et al. 2023). To effectively monitor these changes and develop policies that will protect the environment (Zhao et al. 2024) and promote sustainable development, accurate and current mapping of LULC is therefore necessary. This mapping aids in understanding how changes in land use impact ecosystems, society, and human welfare as well as in projecting future trends (Osman et al. 2023).

Maximum likelihood classification using remote sensing is the most often used method for estimating LULC changes across various spatiotemporal scales (Obeidat et al. 2019; Gitima et al. 2022; Tesfay et al. 2022). However, the amount of time required to process satellite images to generate accurate LULC maps remains a major barrier for researchers studying LULC changes, particularly when using coarse-resolution images (Landsat from the NASA and USGS) (Gomez et al., 2016). Thus, performing LULC classification quickly and accurately is one of the key research areas for remotely sensed images (Batunacun et al., 2018). The Google Earth Engine (GEE) cloud-based computing platform can resolve the most significant problems related to land cover mapping (Phan et al. 2020).

GEE is an open source platform that has a large storage capacity, substantial processing power, and self-programing classification algorithms. These features make it appropriate for thorough and automated LULC classification within study areas (Zhao and Du 2016). Because GEE is not confined to labor-intensive techniques like conversion, mosaics, resampling, projection, and registration (Chowdhuri et al. 2022; Ahmed and Harishnaika 2023), it can evaluate multi-source satellite images quickly and effectively. Machine learning classifiers like RF, SVM, and CART are being used more often on the GEE platform for LULC classification due to their better accuracy and performance (Kelsey et al. 2018; Tassi and Vizzar 2020; Negash et al. 2023). However, there is not much research on comparative performance assessment to inform classifier selection across machine learning types, particularly in Ethiopia (Negash et al. 2023). Moreover, no research has examined the effects of using various input features (spectral bands, spectral indices and topographic variables) on classification precision. This study aims to fill this research gap by comparing three classification algorithms (RF, CART, and SVM) to produce accurate LULC maps and quantify changes in LULC over the previous 30 years. It also looks at how selecting different input features (spectral and auxiliary variables) affect accuracy. In this study the most innovative methodologies, including machine learning and the addition of auxiliary variables to satellite images on GEE platform are used to precisely and swiftly examine LULC changes.

Materials and methods

Description of the study area

The study was conducted at the Robit watershed in northeastern Ethiopia. The study region is situated between 3193 and 1187 m above sea level and is a portion of the upper Awash River basin (Fig. 1). The region experiences 1416 millimeters of annual rainfall on average, with mean minimum and maximum temperatures of 16 and 31 °C, respectively (Tesfay et al. 2022). Eutric cambisols, eutric regosols, and chromc cambisols are the three main types of soil. The Weyna Dega, Dega, and Lower Kolla climates are characteristic of this watershed. The study watershed's lowest sections have pleasant slopes, whereas the

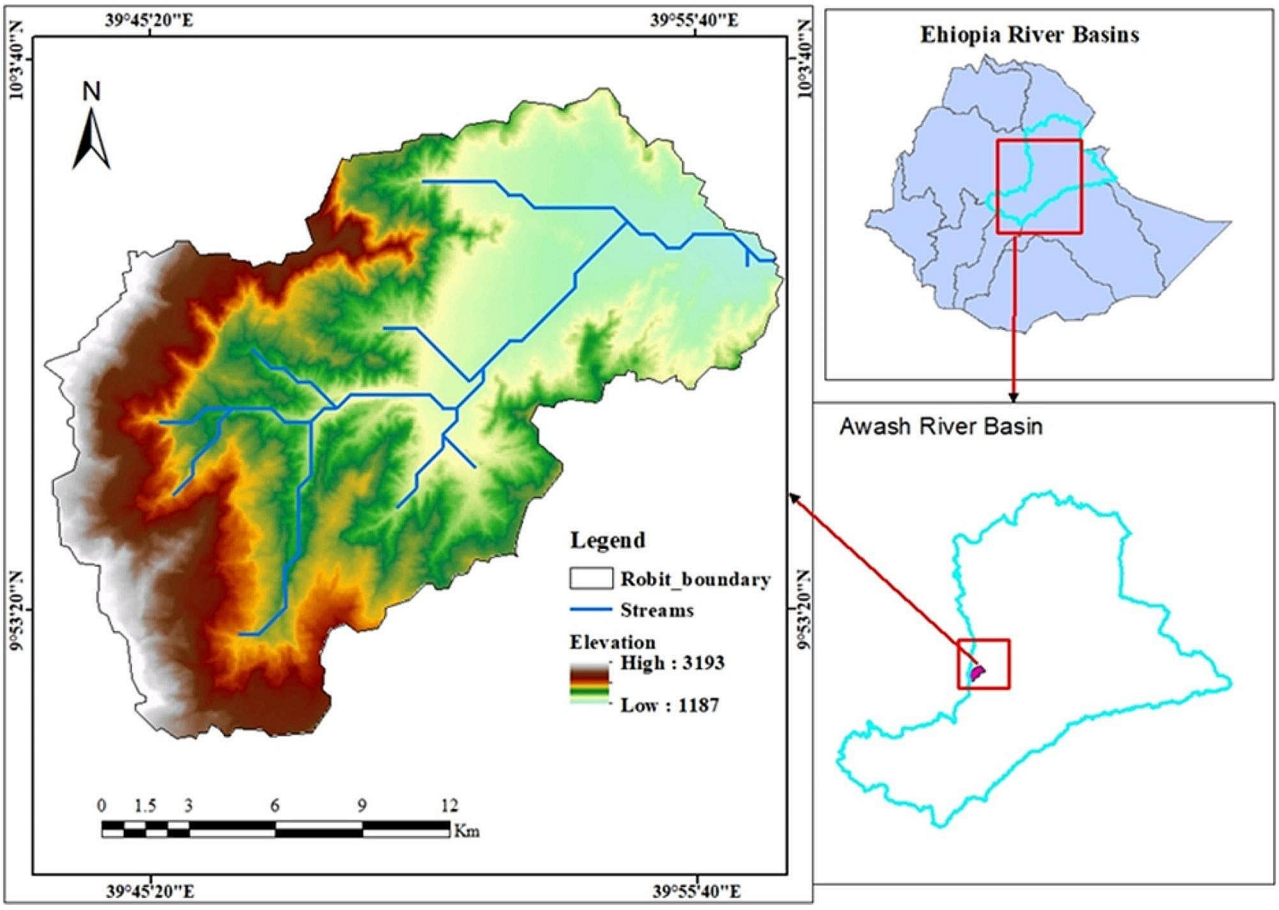

Fig. 1 Location map of the study area

middle and upper areas feature steep slopes and undulating landscapes. The watershed has a great potential for agriculture, particularly in the lower regions. This watershed has a variety of land cover types, including forests, shrublands, grazinglands, and agricultural land. Significant flooding occurs in the lower areas of the watershed during the rainy season, affecting Shewarobit Town, whereas the upper, steeply sloping Robit watershed is severely fragmented (Dejen and Soni, 2021).

Data types and sources

Multi-temporal LULC transformations were discerned using digital data processed from satellite images in the GEE platform. Additional bands for elevation and slope were extracted using the SRTM DEM available through the GEE platform. The classifications of LULC classes by satellite imagery were supplemented with human sensing (complaints of ecological change), Google Earth images, and ground control points (GCP) for verification of each LULC change analysis. Elders' and expert impressions of previous LULC types and their causes of both the past and current forms of LULC shifts in their particular locales within the watershed were employed as human sensing. The data on human sensing were gathered by semi-structured interviews and focus group discussions (FGDs).

Satellite image data

Satellite images were obtained from the publicly accessible GEE data catalog for 1993, 2003, 2013, and 2023 by Landsat 5 Thematic Mapper (TM), Landsat 7 Enhanced Thematic Mapper Plus (ETM+), and Landsat 8 Operational Land Imager (OLI) sensors (Fig. 2). Collection 2 level 2 surface reflectance Landsat images were used; since the images were geometrically, radiometrically, and atmospherically corrected by the image provider (US Geological Survey). Satellite image footprints for the respective years were accessed and clipped to the study watershed. The selection of Landsat images was based on factors such as accessibility, proportion of cloud cover, and association with years of notable events in the research region. Among the remarkable events exclosures were implemented in the study area approximately in 1990 to restore some of the highly deteriorated areas, which might have an effect on LULC (Tesfay et al. 2022). Since Shewarobit Town evolved into Shewarobit Town

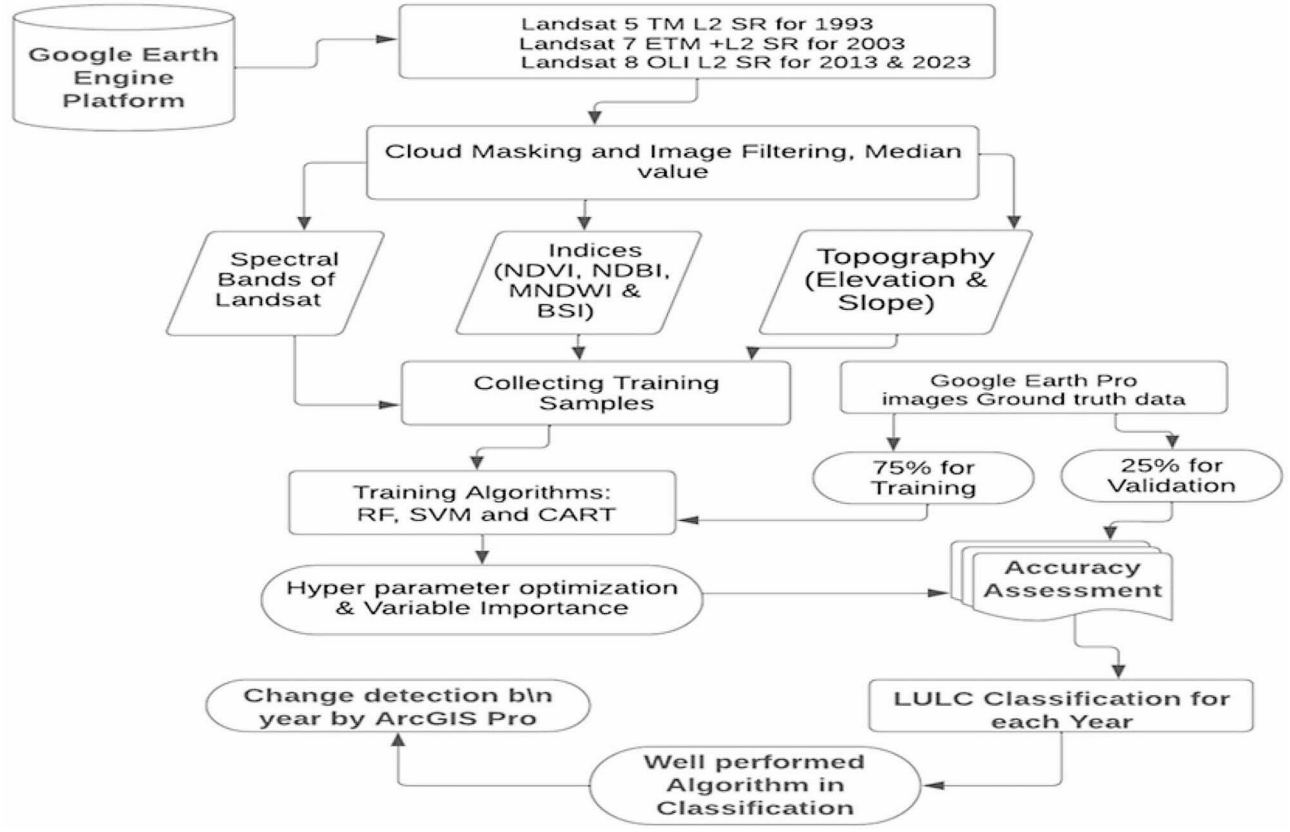

Fig. 2 Flowchart of the LULC classification in google earth engine

Administration in 2013, deforestation has worsened. Furthermore, the 2023 Landsat image was used to depict the existing state of the LULC. Images were collected at intervals of approximately 10 years to clearly show the spatiotemporal changes in the LULC pattern. Every year, no more than 5% of the cloud cover images were chosen using GEE during the months of January, February, and March. Contaminated pixels caused by cloud cover were eliminated from all images using the cloud mask method provided on the GEE. A composite image for the selected years was subsequently generated using the median value, since the median composition methods produced more accurate results in the previous study (Phan et al. 2020).

Auxiliary data

In addition to spectral bands, the following auxiliary datasets were computed to improve the accuracy of land cover classification. Numerous indices, such as the Normalized Difference Vegetation Index (NDVI), Bare Soil Index (BSI), Modified Normalized Difference Water Index (MNDWI), and Normalized Difference Built-up Index (NDBI), were computed using Landsat imagery in the GEE platform (Fig. 2). Different research works have indicated that the integration of topographic characteristics is crucial in identifying and classifying LULC classes, since these variables are associated with the distribution of land cover types (Phan et al. 2020; Nasiri et al. 2022). As a result, the topography-based variables (slope and elevation) were employed as auxiliary variables to incorporate the topography features of the LULC classes throughout the classification process. These generated datasets were then added as new predictor variables to the land cover classifications for each year (Table 1).

Training and validation data

Training and evaluation datasets for LULC mapping were collected from field visits using handheld GPS and internet-based satellite image services. Prior to fieldwork, unsupervised image classification was performed to determine the main LULC classes in the research area. Upon conducting field observations in the study area, six land use land cover types were identified, including agricultural land, bareland, built-up areas, forest, shrubland, and grazingland (Table 2). Ground truth data were then gathered from accessible research areas. Training points that were uniformly distributed around the study region were also gathered using high-resolution satellite images from Google Earth. This approach ensured a diverse and representative sample, thereby enhancing the accuracy and reliability of the LULC classifier. It has been demonstrated that this method of gathering training points

Table 1 Spectral bands, indices, and topograhic metrics used for the LULC classification

Data set (Scenarios)	Variables	Classification Algorithms
Spectral bands	Blue, Red, Green, Near-Infrared, SWIR 1, SWIR 2	RF
		CART
		SVM
Bands + Spectral indices	Blue, Red, Green, Near-Infrared, SWIR 1, SWIR 2 + NDVI BSI, NDWI, NDBI	RF
		CART
		SVM
Bands + Spectral indices + Topographic variables	Blue, Red, Green, Near-Infrared, SWIR 1, SWIR 2 + NDVI, BSI, NDWI, NDBI + Elevation + Slope	RF
		CART
		SVM

Table 2 LULC categories and their description in the study area

Land use/ land cover	General description
Forest	Areas primarily covered with trees that form closed canopies. It includes patches of natural forest and plantations situated in homesteads, farm boundaries, and churches.
Shrubland	Areas dominantly covered by shrub trees (mainly by acacia trees) and sometimes mixed with scattered trees, herbaceous, and grasses.
Grazingland	Areas dominantly covered grasses with only a few widely scattered shrubs and trees, along with exposed areas typically used for grazing.
Agricultural land	Areas covered with annual and perennial crops, and irrigated areas
Built-up Area	Urban areas and other man-made structures, i.e., roads
Bareland	Areas with no vegetation cover consisting of exposed soil mainly river bed

is precise and dependable, and has been widely used and reported in academic publications to obtain LULC classes (Nasiri et al. 2022; Kafle et al., 2023; Osman et al. 2023). A total of 1497data samples based on random sampling were used as training and evaluation datasets. Of the datasets collected, 75% were used for training, and the remaining 25% were used for validation (Fig. 2).

Field survey data

A field survey was conducted to collect GCPs for the identified LULC classes as well as other data regarding LULC classes in the past and changes that have occurred in the research area. The drivers that lead to changes in LULC in the study area have also been understood through the use of these qualitative data. GCPs were collected using a Garmin 60 handheld GPS. Fifty-two respondents were deliberately selected from the high, middle, and lower regions of the watershed to compile historical data on the previous LULC (i.e., 1993, 2003, and 2013) and identify LULC change factors. Elders, carefully selected farmers, and other key informants (such as watershed managers and experts in the field of natural resources) who possessed adequate knowledge of the historical context of the study area were among the research participants. The purposeful selection of informants was based on their substantial experience, distinct perspectives, and profound understanding of the subject matter being studied. The required data were gathered using focus group discussion and semi-structured interview. This data was integrated with the GCPs found using GPS and Google Earth images to create historical LULC maps of the research area.

Image classification and accuracy assessment

The ultimate aim of this work was to increase the accuracy of land cover mapping by employing a novel method. Supervised LULC classification using machine learning classifier in GEE platform was performed. To begin with, watershed boundary and training points for each year were imported into the GEE platform. Prior to classification, the hyper-parameter tuning for RF was assessed to determine the number of trees (ntree) that provide the best accuracy, and an ntree of 10 was used in this study (Fig. 2). The three LULC classifiers that have been recently used by scholars (Ahmed and Harishnaikato, 2023; Negash et al. 2023; Yuh et al. 2023) were then evaluated using similar training data to identify which one produces the best results for Robit watershed. These classifiers are the Classification Regression Trees (CART) technique, Random Forest (RF), and Support Vector Machine (SVM). Lastly, the accuracy of the classifiers for the combination of different variables was evaluated using testing data.

Data from interviews and ground truth data collected at various sample points were used to assess the accuracy of the LULC map. A confusion matrix was used to examine and compare the performance of the LULC maps generated by the three algorithm techniques with

auxiliary variables. Overall accuracy, which indicates the proportion of correctly classified test data, is the most frequently used metric for assessing the effectiveness and accuracy of all classifiers. Therefore, the overall accuracy and Kappa coefficient were calculated (Eqs. 1 & 2) to evaluate the differences in the performance of RF, CART, and SVM in the GEE platform. To assess accuracy across classes, producer and consumer accuracy was also obtained from the confusion matrix using Eqs. 3 and 4 (Nasiri et al. 2022).

$$OA = \frac{Number\ of\ Correctly\ Classified\ Samples}{Number\ of\ Total\ Samples} \quad (1)$$

$$Kappa = \frac{Overall\ Accuracy - Estimated\ Chance\ Agreement}{1 - Estimated\ Chance\ Agreement} \quad (2)$$

$$CA = \frac{Number\ of\ Correctly\ Classified\ Samples\ in\ each\ Class}{Number\ of\ Samples\ Classified\ to\ that\ Class} \quad (3)$$

$$PA = \frac{Number\ of\ Correctly\ Classified\ Samples\ in\ each\ Class}{Number\ of\ Samples\ from\ \mathrm{Reference\ Data\ in\ each\ Class}} \quad (4)$$

LULC change detection

The transition matrix analysis is calculated using the final LULC map, from an accurately classified image. We used ArcGIS Pro to analyze the nature of LULC transitions in the Robit watershed and the transformation of each LULC class. LULC transition maps were produced by using the theme LULC maps of RF from 1993 to 2023. By subtracting the two raster images for the two years, the change in LULC use was calculated and illustrated. This makes it possible to identify the areas where changes in land cover have occurred and their extent and direction. The transition matrix provides an analytical picture of how land cover has changed over time. It also shows the proportion of each land cover class that has changed, remained constant, or completely emerged over a certain period. The percentage and rate of LULC change has been performed by various authors to detect change tendency (Berihun et al. 2019; Yohannes et al. 2020). The following equations were used:

$$Percentage\ of\ LULC\ change\ (\%) = \frac{(Area\ final\ year - Area\ initial\ year)}{Area\ initial\ year}\ x\ 100$$

Area denotes the extent of each LULC class; hence, positive values indicate an increase, whereas negative values imply a decrease.

$$Rate\ of\ LULC\ change\ (ha/year) = \frac{Area\ final\ year - Area\ initial\ year}{Y}$$

Where, Y represents the time interval between the initial and final years.

Variable importance

Variable importance refers to the significance of factors in differentiating the LULC class types. These variable aids in improving classification accuracy by minimizing processing workload and redundancy in the data. The importance of variables in this study was determined using the RF and CART algorithms to estimate the contribution of variables (such as spectral bands, indices, elevation, and slope) to the accuracy of the model that was created. Topographic characteristics are frequently linked to the spatial distribution of LULC classes (Gitima et al. 2022). Accordingly, we consider slope and elevation as terrain features while designing and assessing the LULC models,

Results and discussion

Variables' importance

Variable importance valuation was measured to identify the variables that made the greatest contribution to the identification of LULC classes using the explain technique in the GEE platform. Thus, the importance of characteristic factors was measured for the CART and RF algorithms (Fig. 3). The green band, blue band, and elevation had significance ratings of 49.57, 10.4, and 7.64, respectively, making them the three variables in the CART classifier with the highest effects. The three most important variables in the RF classifier were elevation (10.16), slope (9.70), and red band (8.55). According to Phan et al. (2020) and Nasiri et al. (2022), elevation was found to have significant importance in increasing the accuracy of their classification results in the RF classifier. Since topographic variables determine vegetation, climate, and land cover types in relation to socioeconomic causes, they are therefore more crucial for the identification and classification of LULC in the study area (Birhane et al., 2019).

In both classifiers, bsi, ndbi, and mndwi were the three variables with the lowest level of significance. Phan et al. 2020 also reported that spectral indices were ranked very low in the RF classifier. Because they had no substantial impact on the LULC prediction process, fewer significant components were excluded from consideration in order to enhance predictive performance. The remaining distinguishing characteristics for the LULC grouping had significance values that were somewhat close to one another.

Performance of the classifier with and without auxiliary variables

As explained in the methods section, additional variables have been investigated in addition to the spectral bands

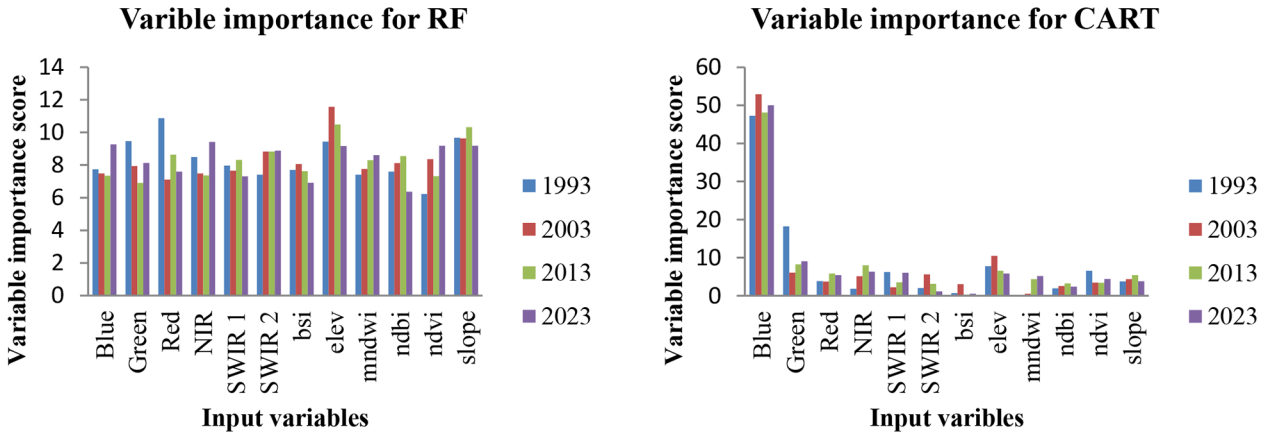

Fig. 3 Variable importance of RF and CART

Table 3 Overall accuracy and kappa coefficient for SVM, CART, and RF before and after the inclusion of additional variables

Year	Classifier	Input			
		Only spectral bands		Spectral bands + Auxiliary Variables	
		OA (%)	K	OA (%)	K
1993	RF	93.34	0.918	94.61	0.935
	CART	88.753	0.864	90.92	0.88
	SVM	50.67	0.428	67.34	0.537
2003	RF	92.32	0.913	93.44	0.927
	CART	89	0.882	91.44	0.90
	SVM	54.98	0.487	65.31	0.545
2013	RF	94.77	0.927	96.53	0.94
	CART	90.836	0.887	92.86	0.918
	SVM	55.6	43.6	69.37	0.595
2023	RF	95.11	0.938	97	0.95
	CART	91.914	0.9	93.33	0.923
	SVM	67	0.573	76	0.67

of Landsat imagery to determine whether they could impact the accuracy of the land cover maps. The findings showed that there was substantial variation between the kappa coefficient and the overall accuracy of RF, CART, and SVM (Table 3). When confined to spectral feature bands, RF achieved the highest average overall accuracy and Kappa coefficient (OA = 93.89%, K = 0.92), whereas CART placed second (OA = 90.13%, K = 0.88). SVM was the least performing classifier, with OA = 57.06% and K = 0.48. Most previous researchers also reported that RF performed better in LULC classification than other machine learning classifiers. In their research, Ahmed and Harishnaikato (2023) examined the classification of Sentinel-2 and Landsat-8 pictures using RF, CART, and SVM. Their findings indicated that RF generated better results and accuracy. Likewise, Yuh et al. (2023) demonstrated that, compared to other classifiers (kNN, SVM, ANN), RF performed the best. The reason for this could be that the two more powerful algorithms "bagging and random" which are referred to as the "powerhouse" of the approach, have helped the RF algorithms (Ahmed and Harishnaikato 2023). The random forest is composed of many decision trees. Choosing the sample and feature subsets to include in the approaches is part of the random operation, which helps to improve generalization ability, increase classification accuracy, and guarantee that each decision tree is independent (Parmar et al. 2019).

Similarly, RF was the best-performing model with OA = 95.6 and K = 0.94, followed by CART (OA = 92.14, K = 0.91), when the auxiliary variables (four spectral indices plus two topographic variables) were included in the classifiers. On the other hand, SVM did not perform the best, with OA = 69.51 and K = 0.58. The outcome showed that when the auxiliary variables were added to the input data for the three classifiers, the OAs and K increased (Table 3) as they enhanced the identification of classes. For example, OA increased in RF and CART by 2.09% and 2.48%, respectively. The impact of auxiliary factors (10 spectral indices + 3 topographic indices) on classification accuracy was also assessed by Phan et al. (2020), who found that the OAs increased, by roughly 4.1–7.7% in RF.

Classifier accuracy assessment at the class level

Producer and consumer accuracies for each of the three classifiers were used to assess class level accuracy (Fig. 4). The RF classifier achieves producer accuracy ranging from 82% for bareland to 95% for shrubland. This means that in the produced LULC map, RF classifies approximately 82% of bareland pixels on the ground as bareland and 95% of the ground's shrubland pixels as shrubland. Consumer accuracy was varied from 82 to 97% for forest and grazingland, respectively. Consumer accuracy represents the possibility that a pixel classified into a particular class truly represents that class on the ground. Therefore, this value indicates that 82% of the grazingland and 97%

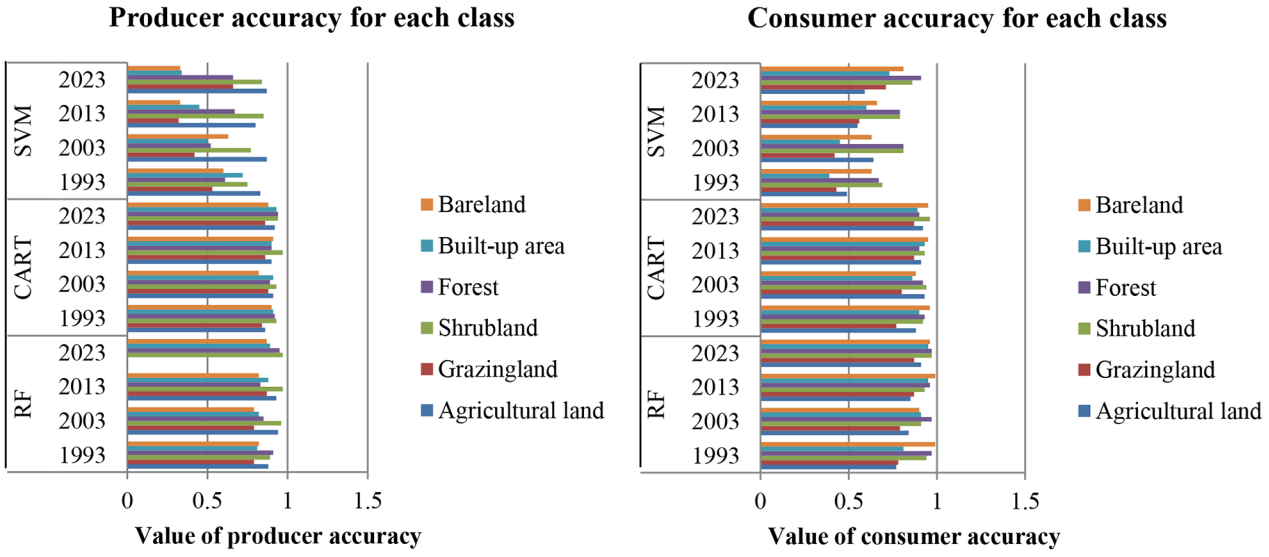

Fig. 4 Producer and consumer accuracy of each class for RF, CART, and SVM

of the forestland on the identified map are found on the ground.

In the CART classifier, the producer's accuracy varies between 86% and 94% for shrubland and grazingland, respectively. The consumer accuracy was 82% for grazingland and 93% for shrubland. SVM obtained low consumer accuracy (53%) and producer accuracy (50%) for grazingland and bareland, respectively. Overall, the results indicate that CART and RF were able to classify the LULC in the study area with a degree of accuracy that was acceptable when compared with the proposed individual accuracies of more than 70%, the overall accuracy of at least 85%, and the kappa coefficient of 75% (Rozenstein and Karnieli 2011; Phan et al., 2020). Although both are within an acceptable range, RF performed better than CART. Conversely, SVM performed the least for LULC classification in this study because it fails to meet the proposed individual accuracy, overall accuracy, and kappa coefficient. Therefore, the SVM classifier is not suitable for LULC classification in the study area.

Classifier-based variation in LULC types' spatiotemporal distribution

The use of different LULC classifiers in this study resulted in varying degrees of LULC classification accuracy, from slight to considerable. Along with the accuracy indicated in the confusion matrix, examining the land cover maps revealed that agricultural land is the predominant LULC type in the research area according to the classification results of RF, CART, and SVM (Fig. 5).

Although there is broad agreement among classifiers regarding agricultural dominance, there was a distinct difference between the areas of each class in the RF, CART, and SVM classification results. The RF-generated maps indicate a consistent distribution of LULC types; however, CART and SVM exhibit inconsistent land cover types for the corresponding years. SVM, for example, generated maps with a greater built-up area in 2003 than 2023. Classifying most agricultural land and barren land as built-up area resulted in the 2003 SVM classifier having a greater built-up area. This outcome completely contradicts the fact that the study area's built-up area has been steadily increasing, as verified by the interpretation of satellite imagery and field survey data. These discrepancies could, of course, result in significant uncertainty for any subsequent application of the map as input (such as estimating soil erosion). This further supports the suggestion that comparing and choosing the best-performing classifier for the study area is essential for accurately classifying land cover. Previous studies have also observed differences in accuracy between classifiers while creating LULC maps (Ahmed and Harishnaika 2023; Negash et al. 2023; Yuh et al. 2023). Yuh et al. (2023) observed that the RF model performed the best and generated highly accurate LULC maps among the models that were compared. The classified map's visual inspection and the accuracy assessment's result's demonstrated that the RF classifier outperformed all other classifiers in this study. Therefore, RF was selected for this study to determine long-term LULC trends for the Robit watershed between 1993 and 2023.

Land use and land cover of the Robit watershed

A precise LULC Map at the watershed level is essential for effective and sustainable land management. Because watershed is a comprehensive natural and man-made

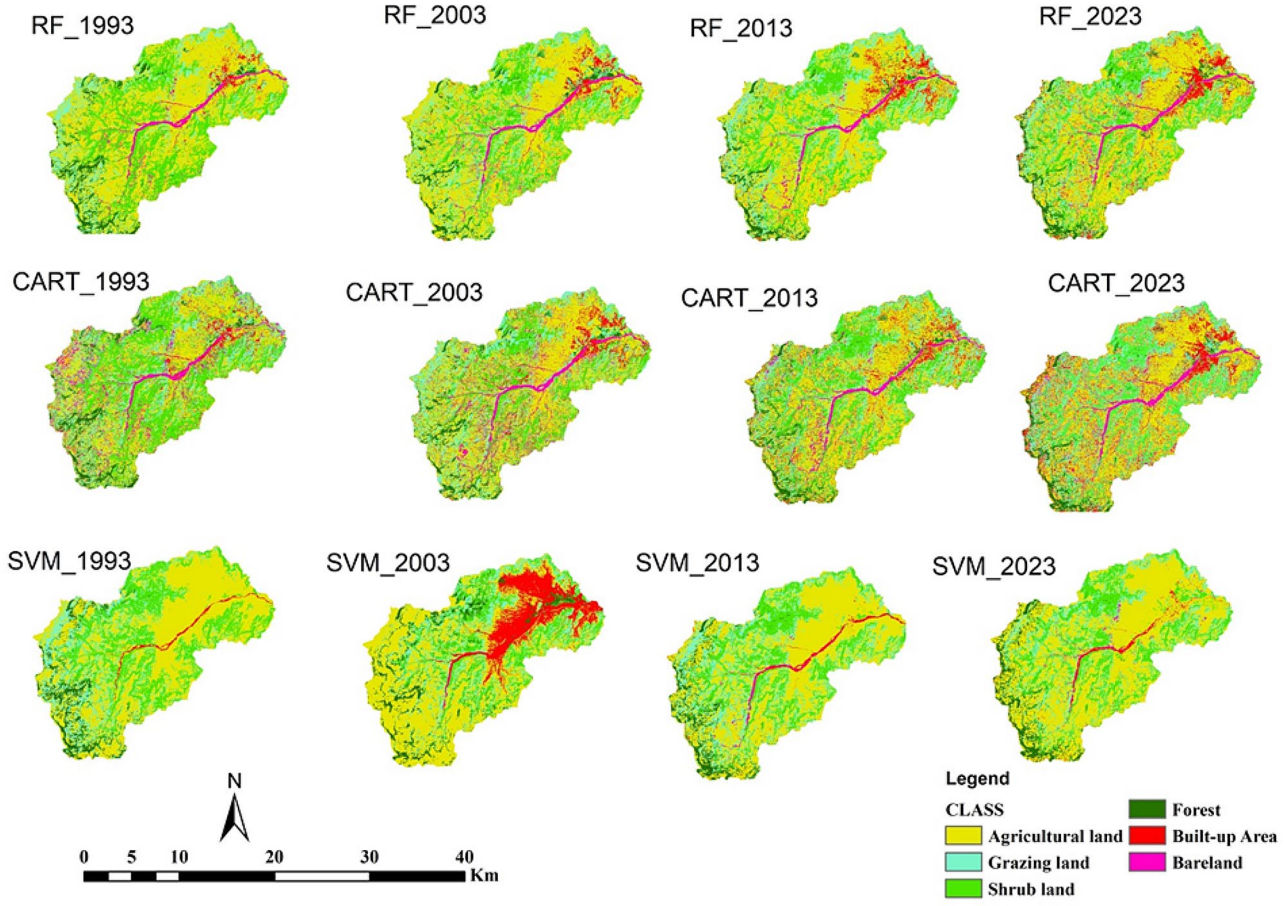

Fig. 5 Comparison of RF, CART, and SVM for the LULC classification

circulation unit, watersheds are effective and suitable for the necessary research to assess this resource, as well as for the planning and implementation of different development projects, such as conservation of soil and water and command area development. Therefore, a comprehensive understanding of LULC dynamics at the watershed level is beneficial for reconstructing previous LULC changes and developing sustainable land resource management plans that protect important landscape functions. Note that the Robit watershed was the site of the LULC investigation for this study. The overall accuracy of the RF classification of LULC images in 1993, 2003, 2013, and 2023 was 93.61%, 93.44%, 96.53%, and 97%, respectively. The total Kappa statistics were found to be 93.5, 92.7, 94, and 95 for the LULC images created in 1993, 2003, 2013, and 2023, respectively. The overall accuracies and Kappa statistics demonstrate that the RF classifier performs better than the SVM and CART algorithms. Therefore, RF classifier was used to create the LULC maps, which show the distribution and trends of LULC in the Robit watershed over a 30- year period. The six classes of land use represented by the LULC maps are agricultural land, built-up areas, barelands, grazinglands, forests, and shrublands (Fig. 6).

In 1993, the majority of the watershed consisted of agricultural land (51.3%) and shrubland (24.5%), with the remaining regions being made up of grazingland (13.9%), forest (5.3%), bareland (3.1%), and built-up areas (1.9%). Agricultural land, shrubland, grazingland and forest accounted for 50%, 20.5%, 18.5%, and 3.8% of the total watershed area in 2003. Of the remaining watershed area comprised bareland and built-up area constituted 4.1% and 3.1%, respectively. In 2013, agricultural land, grazingland, and shrubland accounted for 48.8%, 21.1%, and 19.2% of all land use, respectively. Forest (4.3%), bareland (3.1%), and built-up areas (3.8%), comprised the remaining percentages of the watershed in the same year. Furthermore, in 2023, the most prominent land use types were agricultural land, shrubland, and grazingland and built-up area, comprising 46.6%, 19.8%, 18.8%, and 5.7% of all land use types, respectively. In the same year, the remaining portion of the watershed comprised both forest (5.5%) and Bareland (4.7%).

The results of the LULC maps demonstrate that LULC has undergone significant shifts at various rates during

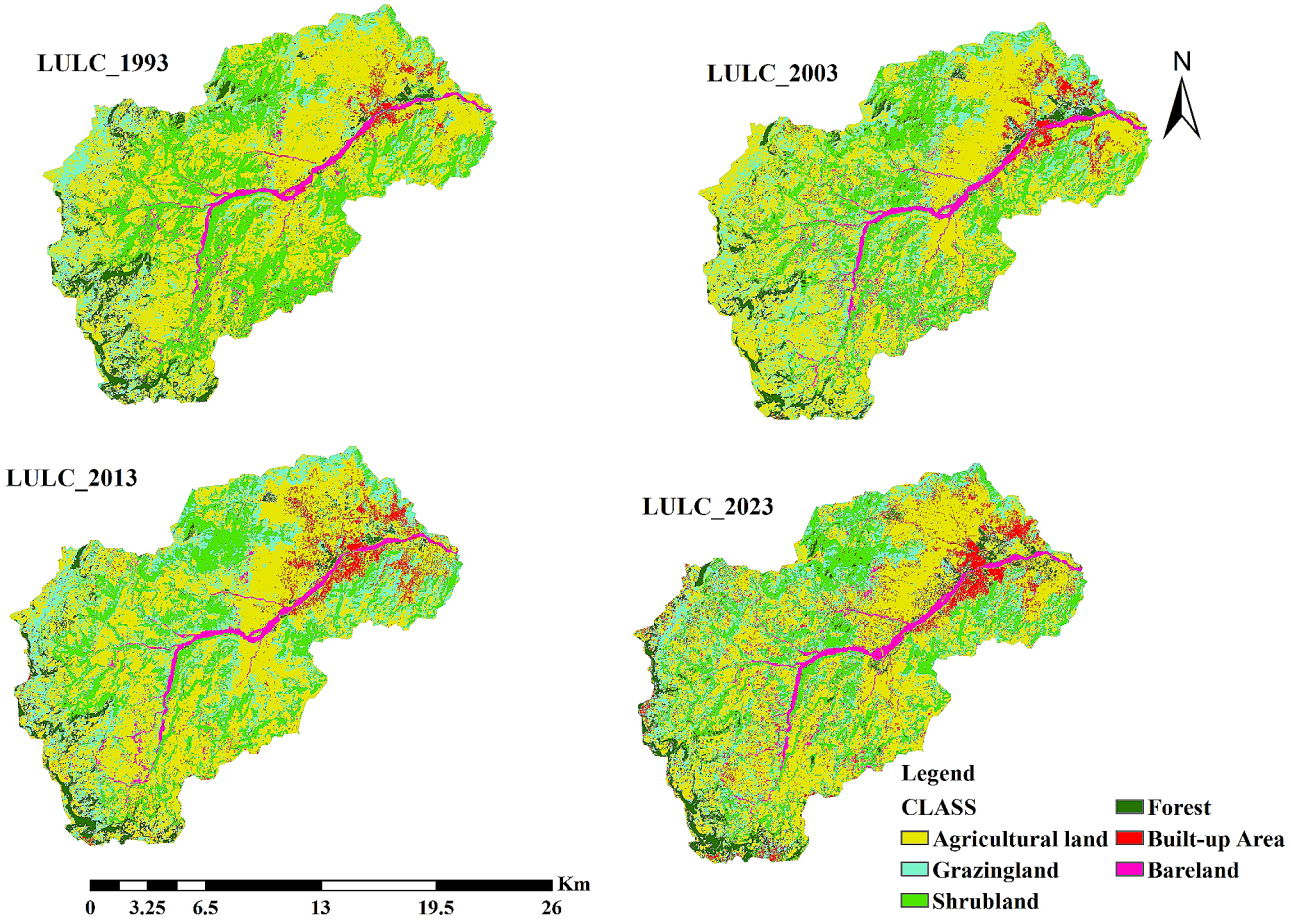

Fig. 6 Spatiotemporal distributions of LULC classes during 1993–2023

Table 4 Distributions and trends of LULC classes during 1993–2023

LULC	1993		2003		2013		2023	
	Area (ha)	%	Area (ha)	%	Area (ha)	%	Area (ha)	%
Agricultural land	15,973	51.3	15,569	50	15,195	48.8	14,518	46.6
Grazingland	4328	13.9	5760	18.5	6570	21.1	5854	18.8
Shrubland	7629	24.5	6383	20.5	5978	19.2	6165	19.8
Forest	1650	5.3	1183	3.8	1339	4.3	1713	5.5
Built-up area	592	1.9	965	3.1	1183	3.8	1775	5.7
Bareland	965	3.1	1277	4.1	965	3.1	1463	4.7
Total	31,137	100	31,137	100	31,137	100	31,137	100

the previous three decades. Similar trends of expansion and shrinkage were observed in the built-up area and agricultural land, respectively. Forest and shrubland has declined over the past 20 years, but it has been rising during the last 10 years. However, over the past 20 years, grazinglands have shown growing tendencies, and over the previous 10 years, they have shown decreasing trends. These findings are consistent with other recent research that has been carried out in Ethiopia; these studies also found that the different land use types had noticeably different LULC change directions during the study period (Yohannes et al. 2020; Gitima et al. 2022; Tesfay et al. 2022; Negash et al. 2023). This indicates that LULC changes are dynamic and nonlinear, meaning that there was no consistent pattern to the conversion of one land use to another. A combination of natural and human causes may be responsible for this disparity (Tolessa et al. 2017).

Expansion of built-up areas and the predominance of agriculture land

Agricultural land was the predominant LULC type with an average coverage of 49.2% in the Robit watershed (Fig. 6; Table 4). There was irrigated agriculture along the

Robit River in addition to rain-fed agriculture. Despite being the dominant class, agricultural land exhibited a consistent slight decline over the study period. Between 1993 and 2003, 2003–2013 and 2013–2023 periods, it was decreased by 2.59, 2.4 and 4.46%, respectively. A total of 15,973 hectares, or 51.3%, of the watershed area was agricultural land in 1993. However, by 2023, this class had substantially declined to 46.6% (14518hectares). The results of this study align with recent LULC analysis studies conducted in Ethiopia (Tesfay et al. 2022; Negash et al. 2023), which found that agricultural land had been the predominant land cover for decades and was beginning to shrink. The majority of the watershed area being used for agriculture may be the result of population growth, which raises the demand for more land for farming. However, the observed reduction in agricultural land may be explained by the growth of built-up areas, which encroach on farmland. Since it produces food, fiber, and other resources, agricultural land is necessary for human survival. Moreover, it provides important ecological benefits like biodiversity, soil fertility, and carbon sequestration (Patel et al. 2024). This decrease might result in food shortages, job losses for farmers and rural communities, and major environmental consequences like soil erosion and climate change. This shows that the environment and human well-being are significantly impacted when agricultural land is lost.

Built-up areas were the land use types in the study area that progressively expanded over the study period. The percentage of land covered by built-up areas increased from 1.9% (592 hectares) in 1993 to 5.7% (1775 hectares) in 2023 (Table 4). During 1993–2003, 2003–2013 and 2013–2023, built-up area increased by 63, 22.6 and 50%, respectively. This expansion of built-up area was mainly at the expanse of agricultural land, as transition matrix indicates. The increase in built-up area represents the fraction of land that increased throughout the research period, even though a substantial portion of it was not covered by constructions. There is a small, denser town in the lower part of the watershed, and some newly built-up such as roads and small villages are growing, as confirmed during the field visit. The information obtained through interviews also verified that Shewarobit's town three kebeles in 1993 had grown to nine kebeles by 2023. The town of Debrisina that was at the upper parts of the watershed also slightly increased. The results of this study are consistent with those of earlier investigations by Haregeweyn et al. (2015) in the Gilgel Tekeze catchment of Northern Ethiopia, Gashaw et al. (2017) in the Andassa watershed of the Blue Nile Basin, Betru et al. (2019) in western Ethiopia, Yohannes et al. (2020) in Beressa watershed and Negash et al. (2023) in the Akaki catchment of Addis Ababa, where significant increases in built-up areas were observed.

Urbanization is a global trend that has a substantial impact on LULC changes (Patel et al. 2024). Urbanization and the growing demand for arable land might exert pressure on forest and woodland use types (Obeidat et al. 2019). In the past few decades, there has been conflict in Ethiopia between the protection of basic arable land and urbanization (Mohamed and Worku 2019). As the field survey and interview revealed, built-up areas including roads and settlements were expanded at the expense of vegetation and agricultural land.

Vegetation dynamics

Shrubland was the second most common LULC at an average of 21%, followed by grazingland (18%) and forest (4.7%). Fluctuations in the dynamics of shrubland, grazingland, and forest cover were documented over the study period. Shrubland declined by 21.6% (1617.6 hectares) between 1993 and 2013, whereas the forest cover declined by 28.3% (439.6 hectares) between 1993 and 2003. There were reductions in shrubs and forests in other LULC change analysis case studies conducted in different parts of Ethiopia. For example, Gashaw et al. (2017) noted a significant decline in the Andassa watershed's shrub and forest cover within the Blue Nile Basin. Gitima et al. (2022) at the Zoa watershed in Southwest Ethiopia also documented a decrease in shrubland from 41.87 to 12.6% throughout the study period. Additionally, there was a decrease in the amount of forest cover in Gubalafito district, Northeastern Ethiopia's between 1986 and 2016 (Abebe et al. 2022). Moreover, the area confined to grazingland increased by 51.8% (2197.3 ha) between 1993 and 2013, but during the subsequent 10 years, it decreased by 10.9%. Grazinglands have increased at the expense of shrublands because of the influx of livestock, which is a crucial component of the farming system.

On the other hand, shrubland expanded by 3% (187 hectares) in 2023, whereas forest cover increased by 44.8% (530 hectares) between 2003 and 2023. The recent increase in shrubland and forests may be attributed to the initiative taken by watershed managers and the Office of Agricultural Development. Regulations concerning land use and management have been in effect in the research region since 2017. Experts evaluated the land's potential by considering several factors, including the slope and characteristics of the soil. Following training, farmers begin using their land according to the land capability assessment, which leads to the proper use of land. Vegetation increase may also result from the exclusion of human and domestic animal involvement (area exclosures). According to information gathered from interviews and field observations, area exclosures were put into place in both high elevations mountain regions where forests predominated and lower and intermediate watershed regions where shrubs predominated. The

spread of plantations primarily composed of Eucalyptus species, at higher elevations may also contribute to the increase in vegetation. This is because Eucalyptus plantations are more economically significant because of their fast-growing nature and increased market demand. Similar to this study, Negash et al. (2023) stated that in the Akaki catchment of Ethiopia, the forest area increased from 4.65% (67.68 km2) in 1990 to 10.09% (146.85 km2) in 2020. Furthermore, according to Abebe et al. (2022), bush land expanded from 14.8 to 21% in Gubalafito district during the study period.

The Normalized Difference Vegetation Index (NDVI) value varies from −0.033 to 0.5 between 1993 and 2023 (Fig. 7). According to the NDVI study, in 1993, values between 0.27 and 0.36 prevailed, whereas in 2023, values between 0.015 and 0.14 dominated. This suggests that 2023 saw a decrease in vegetation, especially shrubland, whereas 2023 saw a slight increase in forest cover, as indicated by the NDVI value rising from 0.36 to 0.5. In addition, in 2023, the NDVI value in the bottom part of the watershed was from 0.18 to 0.27, indicating a rise in grazingland.

Bareland expansion

Bareland, which primarily represents the river bed, had the lowest level of domination in the research region, with an average of 3.56%. The LULC change analysis showed that in 1993, the watershed's percentage of bareland was the lowest (3.1%). However, its coverage gradually increased by 51.6% between 1993 and 2023 (Table 4). River bed cover expands primarily at lower elevations within the watershed. A LULC change analysis conducted in the Gilgel Tekeze watershed in north Ethiopia also revealed a slight increase in the percentage of riverbed cover and bare land, of 0.2% and 0.4%, respectively (Haregeweyn et al. 2015).

Land use land cover change detection

There was gain and loss among the different LULC types from 1993 to 2023 (Fig. 8), according to the LULC change detection analysis conducted using ARC GIS PRO. Agricultural land and shrubland areas showed a net negative change, while built-up area, grazingland and bareland underwent the largest net positive change, as illustrated in Fig. 8.

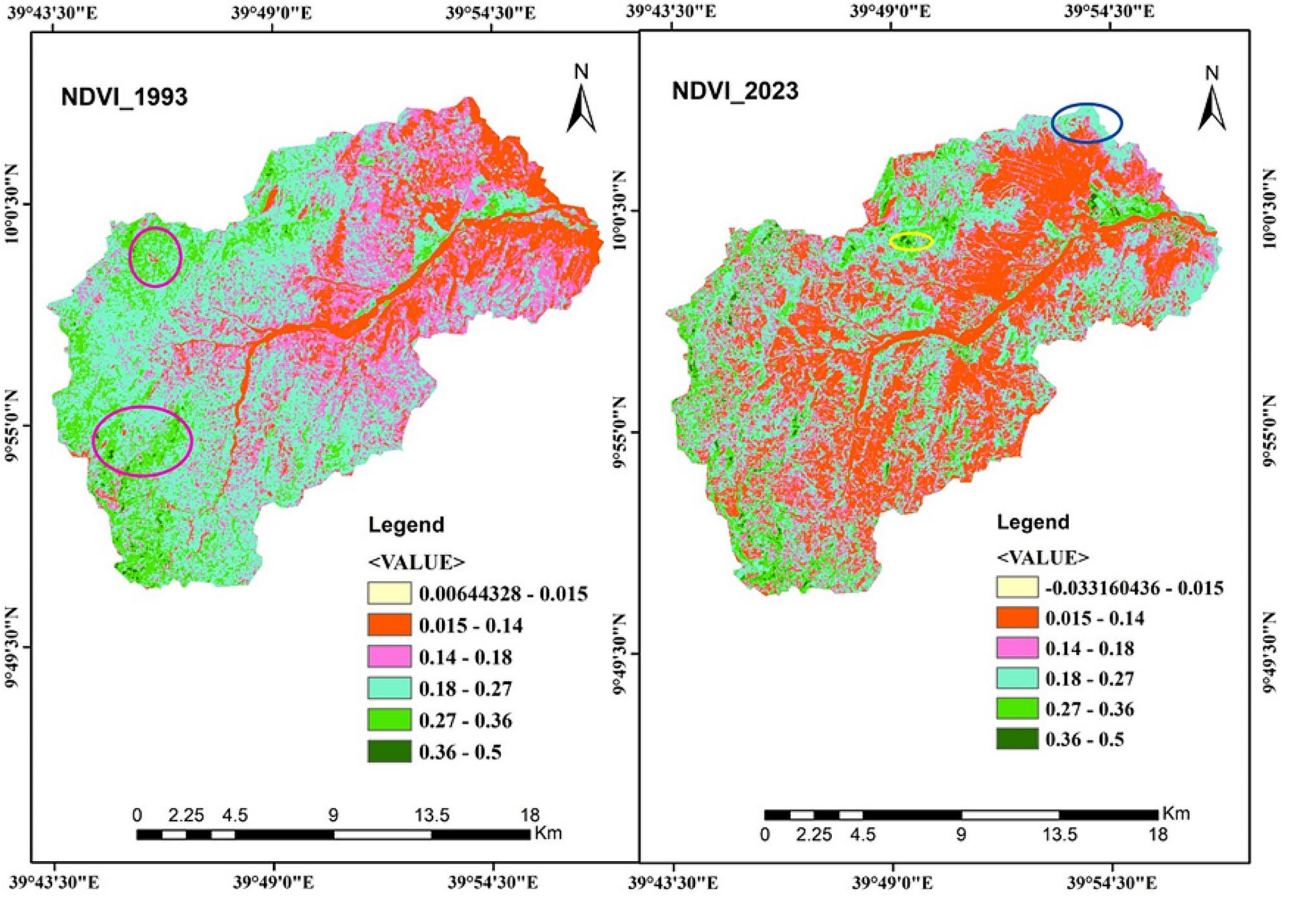

Fig. 7 NDVI map between 1993 and 2023

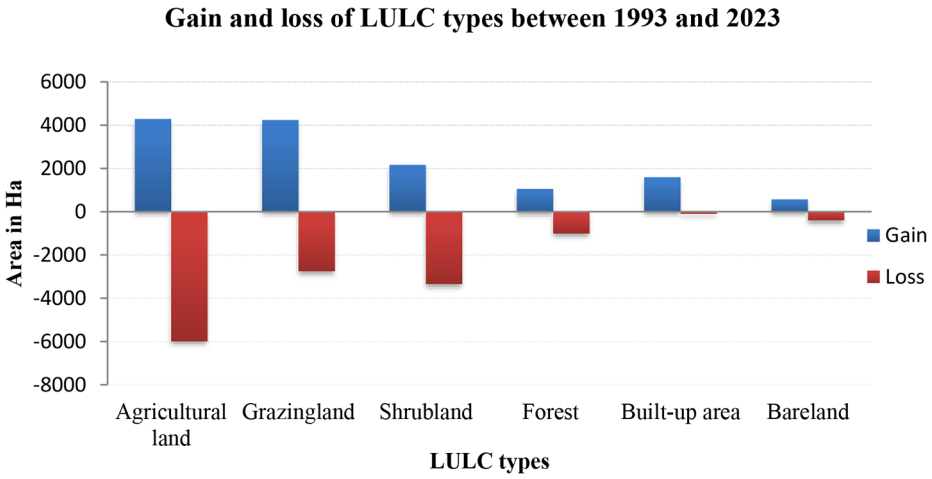

Fig. 8 Gain and loss of LULC types between 1993 and 2023

Table 5 Results of analysis of the LULC change matrix from 1993 to 2023

LULC types	Agricultural land	Grazingland	Shrubland	Forest	Built-up area	Bareland
Agricultural land	31.8	8.89	4.03	1.73	4	0.91
Grazingland	5.49	5	1.62	0.85	0.71	0.28
Shrubland	5.49	4.13	12.75	0.73	0.21	0.32
Forest	1.24	0.53	1.29	2.02	0.15	0.08
Built-up area	0.33	0.09	0.02	0.08	0.52	0.21
Bareland	0.87	0.15	0.078	0.03	0.16	1.77

Approximately 53% of LULC remains the same, whereas 47% of class types change between 1993 and 2023. The transition between grazing and agricultural land has been one of the most noticeable changes. Approximately 8.89% of the agricultural land has been transformed into grazingland, and 5.49% of the pasture has been returned to agricultural use (Table 5). During the interviews with the chosen respondents, such conversion of land between grazing and agricultural use was also confirmed. They said that after agricultural land's productivity declined, it was fallowed and used for grazing for a few years. When their arable land was lost owing to a decline in productivity, additional grazing land was also turned into agricultural land. Osman et al. (2023) suggested that the seasonality of grass may have an impact on the intensity of active losses and gains in grazing land. The results of Gashaw et al. (2017), who found a notable conversion of grassland and cultivated land between each other, are likewise in line with this finding. For instance, they claimed that between 2000 and 2015, 2484 hectares of grassland were changed back to cultivated land and 1969 hectares of cultivated land were returned to grassland areas. Additionally, in this study, 5.49% of the shrubland was converted to agricultural land. The study carried out by Gitima et al. in 2022 at the Zoa watershed in Southwest Ethiopia also reported on the expansion of agricultural land at the expense of shrubland.

The study area's 4% increase in built-up area over agricultural land between 1993 and 2023 was another prominent change that was noticed. Respondents claimed that more productive agricultural land was cleared for town growth, especially that dominated by perennial crops like oranges and mangoes.

Drivers of LULC changes in the study area

According to data gathered from key informants (KII) interviews and focused group discussion (FGD), several factors that cause LULC dynamics were identified in the Robit watershed. Population growth, expansion of built-up areas, illegal settlement, agricultural land expansion, fuelwood collection, charcoal production, land redistribution, and intervention (land use and management rules and area exclosure) were among the factors causing LULC shifts. The majority of respondents (96%) believed that the expansion of agricultural land was the foremost driver of LULC dynamics. This is supported by the LULC analysis, which showed that agricultural land covers approximately 49.2% of the watershed area. Besides, the summary of the FDGs revealed that the domination of agricultural land is due to a decline in land productivity and population growth that pushes people to need more land. In recent years, there has been a notable increase in population in the two districts that encompass the Robit watershed. According to the Central

Statistical Agency of Ethiopia (CSA) national census report, the total population of Kewet woreda was 107,644 in 1994. However, in 2007, the woreda's population increased to 118,333, indicating a 9.97% increase from the 1994 census. Likewise, the population is expected to reach 147,093 in 2017. Tarmaber woreda had 84,481 residents in 2007; by 2017, that number was expected to rise to 103,618 (CSA 2013). The watershed, especially its lower regions, has the ability to produce cash crops like tobacco, mungbean, and onions; as a result, the farmland has mostly expanded into grazing and shrubland. Many studies have also reported that agricultural growth that trigger by population growth is a key factor in changes in LULC (Berihun et al. 2019; Degife et al. 2019; Abebe et al. 2022; Gitima et al. 2022).

Nearly 94.2% of the respondents stated that illegal settlement and growing built-up areas were important drivers of LULC dynamics. This is corroborated by the LULC analysis, which shows that the built-up area increased from 1.9 to 5.7% between 1993 and 2023. During the field visit, it was determined that huge agricultural regions covered in perennial plants, such as orange and mango, were being turned into settlements. According to experts, unlawful settlement is one of the key elements influencing the application of land use and management regulations, which promise strategies for lowering adverse LULC dynamics. Similarly, prior studies have reported that illegal settlement and expansion of built- up area at the expanse of agricultural land was the driving factor causing LULC changes (Tolessaa et al., 2017).

According to 88.5% of respondents, the logging of wood for fuel and charcoal production was a significant factor impacting the LULC change in the watershed. Acacia species are preferred for producing charcoal because they are more common in the lower part of the watershed. Additionally, the FGD confirmed that the wood is primarily collected by the watershed's rural residents for fuel and charcoal. For financial benefit, they also sold wood and charcoal to the town's residents. The majority of inhabitants in the upper watershed also rely on the sale of firewood for locally crafted furniture, and construction needs, making trees their main source of revenue. Owing to this demand, woodlots with eucalyptus trees and plantations, even on agricultural land, were mostly found in the upper regions of the watershed. Tadese et al. (2021) noted that the removal of trees and timber for residential and commercial usage is another significant issue that contributes to LULC changes. Moreover, approximately 71% of the interviewees specified that area exclosure was considered the driver of LULC change. FGD also asserted that area exclosure courage's that increasing of vegetation.

Conclusions

The management of LULC can be directly affected by the accuracy of classification algorithms, making it a critical component of remote sensing analysis. Therefore, choosing the best performing classification algorithm is a critical step, and the accuracy of this process is vital for effective LULC change analysis. In this study, the accuracy of the three algorithms (CART, RF and SVM) for LULC classification in the study area is compared in Google Earth Engine Platform. Additional input datasets, including, spectral indices, and topographic characteristics, were incorporated in to satellite images to increase accuracy. The results demonstrated that RF could obtain excellent accuracy with OA=95.6 and K=0.94 when topographic variables and spectral indices were added to the images. The result of this study clearly showed that choosing a single classification technique is insufficient to produce a land cover map that is both highly accurate and realistic. Therefore, it is crucial to compare and choose the superior one for a specific study area.

Spatiotemporal analysis of land cover and land use types changes from 1993 to 2023 was conducted using RF at the Robit watershed in northeastern Ethiopia. The result showed that there were significant spatiotemporal differences in LULC changes in the Robit watershed during the past 30 years. Agricultural land was the most prominent kind of LULC, with a dropping tendency, while built-up areas consistently showed an increasing pattern. After 20 years of declining trend, the vegetation area (forest and shrubland) has recently shown an increasing tendency. Bareland shows an increasing trend, whereas grazingland shows a growing trend with a current diminishing tendency. The largest changes in land use were observed to be occurring from shrubland to agricultural land and from agricultural land to built-up areas. The observed changes in LULC in the study region are mostly associated with population growth, the growth of agricultural land, the collection of fuelwood, the production of charcoal, the expansion of built-up areas, illegal settlement, and intervention. This study provides information about LULC patterns in Robit watershed that could be useful for creating management plans and regulations for evaluating and monitoring the natural resources in the watershed. Thereby, this information is essential for protecting one of Ethiopia's most significant landscapes.

Acknowledgements

The authors would like to thank Dire Dawa University and Addis Ababa University for their assistance in this study. We appreciate the assistance of the Robit Watershed residents in sharing their data and experiences. The authors express their sincere gratitude to the USGS for providing Landsat datasets at no cost, as well as to Google Earth Engine Platform for providing such a powerful free cloud system for image processing analysis.

Author contributions
Author contribution statement Weyenshet Tesfaye: collect the data, analysis, and preparation and wrote manuscript Eyasu Elias: study's concept and design and wrote manuscript Bikila Warkineh: study's concept and design and wrote manuscript Meron Tekalign: study's concept and design and wrote manuscript Gebeyehu Abebe: study's concept and design, data analysis and wrote manuscript.

Funding
No external funding was received during the study time.

Data availability
No datasets were generated or analysed during the current study.

Declarations

Ethics approval and consent to participate
Not applicable.

Competing interests
The authors declare no competing interests.

Received: 15 May 2024 / Accepted: 31 July 2024
Published online: 14 August 2024

References

Abd El-Hamid HT, Caiyong W, Hafiz MA, Mustafa EK (2020) Effects of land use/land cover and climatic change on the ecosystem of North Ningxia, China. Arab J Geosci 13:1–13
Abebe G, Getachew D, Ewunetu A (2022) Analysing land use/land cover changes and its dynamics using remote sensing and GIS in Gubalafito district, Northeastern Ethiopia. SN Appl Sci 4(1):30
Ahmed SA, Harishnaika N (2023) Land use and land cover classification using machine learning algorithms in Google earth engine. Earth Sci Inf, 1–17
Batunacun, Nendel C, Hu Y, Lakes T (2018) Land-use change and land degradation on the Mongolian Plateau from 1975 to 2015—A case study from Xilingol, China. Land Degrad Dev 29(6):1595–1606
Berihun ML, Tsunekawa A, Haregeweyn N, Meshesha DT, Adgo E, Tsubo M, Yibeltal M (2019) Exploring land use/land cover changes, drivers and their implications in contrasting agro-ecological environments of Ethiopia. Land use Policy 87:104052
Birhane E, Ashfare H, Fenta AA, Hishe H, Gebremedhin MA, Solomon N (2019) Land use land cover changes along topographic gradients in Hugumburda national forest priority area, Northern Ethiopia. Remote Sens Appl: Soc Environ 13, 61–68
Betru T, Tolera M, Sahle K, Kassa H (2019) Trends and drivers of land use/land cover change in Western Ethiopia. Appl Geogr 104:83–93
Chowdhuri I, Pal SC, Saha A, Roy P, Chakrabortty R, Shit M (2022) Application of novel framework approach for assessing rainfall induced future landslide hazard to world heritage sites in indo-Nepal-Bhutan Himalayan region. Geocarto Int 37(27):17742–17776
CSA (2013) *Population projection of Ethiopia for all regions at Wereda level from 2014–2017* (issue August 2013). Federal Democratic Republic of Ethiopia Central Statistical Agency (CSA)
Degife A, Worku H, Gizaw S, Legesse A (2019) Land use land cover dynamics, its drivers and environmental implications in Lake Hawassa Watershed of Ethiopia. Remote Sens Appl: Soc Environ 14:178–190
Dejen A, Soni S (2021) Flash flood risk assessment using geospatial technology in Shewa Robit town, Ethiopia. Model Earth Syst Environ 7, 2599–2617
Gashaw T, Tulu T, Argaw M, Worqlul AW (2017) Evaluation and prediction of land use/land cover changes in the Andassa watershed, Blue Nile Basin, Ethiopia. Environ Syst Res 6(1):1–15
Gitima G, Teshome M, Kassie M, Jakubus M (2022) Spatiotemporal land use and cover changes across agroecologies and slope gradients using geospatial technologies in Zoa watershed, Southwest Ethiopia. Heliyon, 8(9)
Gómez C, White JC, Wulder MA (2016) Optical remotely sensed time series data for land cover classification: a review. ISPRS J Photogrammetry Remote Sens 116:55–72
Haregeweyn N, Tesfaye S, Tsunekawa A, Tsubo M, Meshesha DT, Adgo E, Elias A (2015) Dynamics of land use and land cover and its effects on hydrologic responses: case study of the Gilgel Tekeze catchment in the highlands of Northern Ethiopia. Environ Monit Assess 187:1–14
Johnson BG, Zuleta GA (2013) Land-use land-cover change and ecosystem loss in the Espinal ecoregion, Argentina. Agric Ecosyst Environ 181:31–40
Kelsey EN, Grant EG, Nikolay IS, Ryan NE, Dmitry AS (2018) Land cover change in the lower Yenisei river using dense stacking of Landsat imagery in Google earth engine. Remote Sens 10(8):1226. https://doi.org/10.3390/rs10081226
Kidane M, Bezie A, Kesete N, Tolessa T (2019) The impact of land use and land cover (LULC) dynamics on soil erosion and sediment yield in Ethiopia. Heliyon, 5
Kleemann, J, Baysal G, Bulley HN, Fürst C (2017) Assessing driving forces of land use and land cover change by a mixed-method approach in north-eastern Ghana, West Africa. J Environ Manage, 196, 411–442
Mohamed A, Worku H (2019) Quantification of the land use/land cover dynamics and the degree of urban growth goodness for sustainable urban land use planning in Addis Ababa and the surrounding Oromia special zone
Nasiri V, Deljouei A, Moradi F, Sadeghi SMM, Borz SA (2022) Land use and land cover mapping using Sentinel-2, Landsat-8 Satellite Images, and Google Earth Engine: A comparison of two composition methods. Remote Sensing, 14(9), 1977
Negash ED, Asfaw W, Walsh CL, Mengistie GK, Haile AT (2023) Effects of land use land cover change on streamflow of Akaki catchment, Addis Ababa, Ethiopia. Sustainable Water Resour Manage 9(3):78
Nigussie Z, Tsunekawa A, Haregeweyn N, Adgo E, Nohmi M, Tsubo M, Abele S (2017) Factors affecting small-scale farmers' land allocation and tree density decisions in an acacia decurrens-based taungya system in Fagita Lekoma District, North-Western Ethiopia. Small-Scale Forestry 16:219–233
Obeidat M, Awawdeh M, Lababneh A (2019) Assessment of land use/land cover change and its environmental impacts using remote sensing and GIS techniques, Yarmouk River Basin, north Jordan. Arab J Geosci 12:1–15
Osman MA, Abdel-Rahman EM, Onono JO, Olaka LA, Elhag MM, Adan M, Tonnang HE (2023) Mapping, intensities and future prediction of land use/land cover dynamics using Google earth engine and CA-artificial neural network model. PLoS ONE, 18(7), e0288694
Parmar A, Katariya R, Patel V (2019) A review on random forest: An ensemble classifier. In International conference on intelligent data communication technologies and internet of things (ICICI) 2018 (pp. 758–763). Springer International Publishing
Patel A, Vyas D, Chaudhari N, Patel R, Patel K, Mehta D (2024) Novel approach for the LULC change detection using GIS & Google Earth Engine through spatiotemporal analysis to evaluate the urbanization growth of Ahmedabad city. Results Eng 21:101788
Pereira C, Tsikata D (2021) Contextualising Extractivism in Africa. Feminist Afr 2(1), 14–48. https://www.jstor.org/stable/48725692
Phan TN, Kuch V, Lehnert LW (2020) Land cover classification using Google Earth Engine and random forest classifier—the role of image composition. Remote Sens 12(15):2411
Rozenstein O, Karnieli A (2011) Comparison of methods for land-use classification incorporating remote sensing and GIS inputs. Appl Geogr 31(2):533–544
Tadese S, Soromessa T, Bekele T (2021) Analysis of the current and future prediction of land use/land cover change using remote sensing and the CA-markov model in Majang forest biosphere reserves of Gambella, southwestern Ethiopia. Sci World J 2021:1–18
Tassi A, Vizzari M (2020) Object-oriented LULC classification in Google earth engine combining SNIC, GLCM, and machine learning algorithms. Remote Sens 12(22):3776
Tesfay F, Kibret K, Gebrekirstos A, Hadgu KM (2022) Land use and land cover dynamics and ecosystem services values in Kewet district in the central dry lowlands of Ethiopia. Environ Monit Assess 194(11):801
Tolessa T, Senbeta F, Kidane M (2016) Landscape composition and configuration in the central highlands of Ethiopia. Ecology Evol 6(20), 7409–7421
Tolessa T, Senbeta F, Kidane M (2017) The impact of land use/land cover change on ecosystem services in the central highlands of Ethiopia. Ecosyst Serv 23:47–54
Winkler K, Fuchs R, Rounsevell M, Herold M (2021) Global land use changes are four times greater than previously estimated. Nat Commun 12(1):2501
Yeshaneh E, Wagner W, Exner-Kittridge M, Legesse D, Blöschl G (2013) Identifying land use/cover dynamics in the Koga catchment, Ethiopia, from multi-scale data, and implications for environmental change. ISPRS Int J Geo-Information 2(2):302–323

Yohannes H, Soromessa T, Argaw M, Dewan A (2020) Changes in landscape composition and configuration in the Beressa watershed, Blue Nile basin of Ethiopian highlands: historical and future exploration. Heliyon, *6*(9)

Yuh YG, Tracz W, Matthews HD, Turner SE (2023) Application of machine learning approaches for land cover monitoring in northern Cameroon. Ecol Inf 74:101955

Zhao W, Du S (2016) Learning multiscale and deep representationsfor classifying remotely sensed imagery. ISPRS J PhotogrammRemote Sens 113:155–165

Zhao Z, Islam F, Waseem LA, Tariq A, Nawaz M, Islam IU, Hatamleh WA (2024) Comparison of three machine learning algorithms using Google earth engine for land use land cover classification. Rangel Ecol Manage 92:129–137

Publisher's Note